

## A New Spallation Ultracold Neutron Source at RCNP

S. Kawasaki<sup>†</sup>, Y. Masuda<sup>†</sup>, S.C. Jeong<sup>†</sup>, Y. Watanabe<sup>†</sup>, K. Matsuta\*,  
M. Mihara\*, K. Hatanaka\*\*, R. Matsumiya\*\*

<sup>†</sup> *High Energy Accelerator Research Organization (KEK), 1-1 Oho, Tsukuba,  
Ibaraki 305-0801, Japan*

\* *Dept. of Physics, Osaka Univ., Toyonaka Osaka560-0043, Japan*

\*\* *RCNP, Osaka Univ., 10-1 Mihogaoka, Ibaraki, Osaka 567-0047, Japan*

### Abstract

A spallation ultracold neutron source has been developed at RCNP, Osaka University, Japan. Superfluid helium is used for a UCN converter. First UCN were produced at 2002. At that time, UCN density was 0.7 UCN/cm<sup>3</sup>. Improving superfluid helium temperature, cleaning of an inner wall of a helium container and so on, the UCN density has increased up to 26 UCN/cm<sup>3</sup> with maximum energy of 90 neV.

A new UCN source has been developed. A main improvement is a horizontal extraction. With other improvements, the UCN density will be five times as much as the former UCN source.

## 1 Introduction

Ultra cold neutrons (UCN) are very low energy neutrons which have a energy of about 100 neV, a velocity of about 5 m/s and a wavelength of about 50 nm [1]. They feel gravity, magnetic force, weak and strong interaction. According to their long wave length, UCN feel average potential of a material. This is called Fermi potential.

Since some materials have the Fermi potential larger than 100 neV, UCN are totally reflected at their surface. Thus UCN can be confined in a material bottle. These confined UCN are used for various experiments such as a neutron electric-dipole moment search [2], a gravity experiment [3], a neutron life time measurement [4] and so on. In these experiments, high UCN density is essential.

## 2 UCN production with super-fluid helium

UCN production by phonon excitation in superfluid helium (He-II) was proposed by Golub and Pendlebury in 1977 [5]. Since a large phonon phase space can be used, the phase-space density of the neutron is greatly enhanced upon phonon excitation. Therefore it is free from a limitation of Liouville's theorem.

Solid deuterium is also used for production of UCN. An advantage of solid deuterium is large production rate  $P$ . On the other hand, the He-II has long neutrons storage time  $\tau_s$ . The UCN density is represented by the product of  $P$  and  $\tau_s$ .

Since  $^4\text{He}$  do not absorb neutrons,  $\tau_s$  in He-II depends on phonon up-scattering rate. It depends on He-II temperature.  $\tau_s$  is 36 s and 600 s at 1.2 K and 0.8 K, respectively. In order to achieve long  $\tau_s$ , it is important to keep helium temperature below 1 K.

## 3 Current UCN source at RCNP

A spallation UCN source has been developed at RCNP, Osaka University, Japan. First UCN were produced at RCNP at 2002 [6]. At that time, only a  $^4\text{He}$  cryostat was used. He-II temperature was 1.2 K and the  $\tau_s = 14$  s

In order to keep He-II temperature below 1 K, a  $^3\text{He}$  cryostat was developed. Avoiding from a heat load connecting about superfluid film flow, a perimeter of a He-II bottle was reduced. As a result, He-II temperature was down to 0.8 K. Surface condition of the He-II bottle and the UCN guide is also important to achieve long  $\tau_s$ . Alkali cleaning to remove oil component and baking to remove moisture was conducted. Thus,  $\tau_s$  became as long as 81 s in 2011. UCN density of 26 UCN/cm<sup>3</sup> with maximum energy of 90 neV are available [7].

### 3.1 Spallation UCN source

Figure 1 shows the layout of the UCN source. The He-II is surrounded by the liquid and solid D<sub>2</sub>O moderators. The solid D<sub>2</sub>O moderator is kept cooling at 20 K by a GM cryostat. These are located just above a spallation target. Spallation neutrons are firstly moderated in the liquid and solid D<sub>2</sub>O, then transfer their energy to phonon of He-II and become UCN. Since distance between the spallation target and the He-II is close, UCN are produced effectively.

The He-II bottle consist of an aluminum tube with a thickness of 2 mm, a diameter of 16 cm and a length of 41 cm. The volume of He-II is 8 liter. The inner wall of the bottle is coated with nickel by applying electro-less plating. The Fermi potential of the nickel plating is 210 neV.

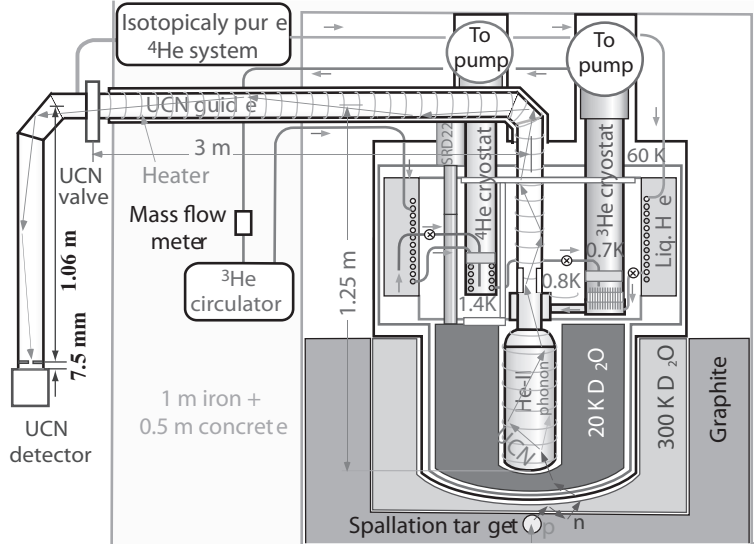


Figure 1: Current UCN source at RCNP

## 3.2 UCN production

### 3.2.1 Simulation

Cold neutron flux is estimated by Monte Carlo simulation. PHITS simulation code is used. This code assume the solid  $D_2O$  of 20 K is a ideal gas. The calculated flux at resonant energy of single-phonon excitation is  $d\phi(E)/dE = 9.3 \times 10^8 \text{ n/cm}^2/\text{meV/s}$  for proton beam power of  $400 \text{ MeV} \times 1 \mu\text{A}$ . The production rate of UCN with maximum energy of 210 neV, which is container Fermi potential, is calculated to  $9 \text{ UCN/cm}^3/\text{s}$  for a single-phonon excitation and  $14 \text{ UCN/cm}^3/\text{s}$  for including multi-phonon excitation [8]. However, the ideal gas assumption in the simulation is not sufficient. Deuterons and oxygen nuclei are strongly bound in the solid  $D_2O$ . Therefore the effective mass for cold neutron scattering are larger and the neutron temperature is higher, for example, 50 K [9]. At the temperature of 50 K and 80 K, the

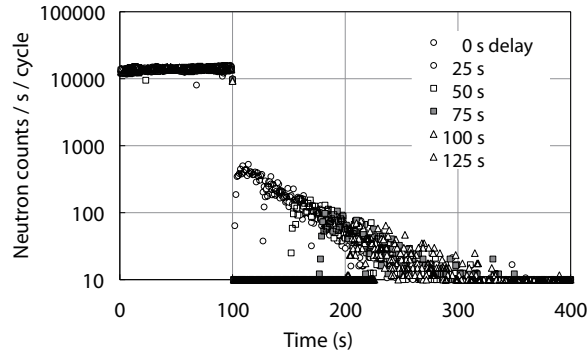


Figure 2: Storage time measurement. Proton beam of  $400 \text{ MeV} \times 0.2 \mu\text{A}$  is impinged for 100 s. UCN counts for each time delay after valve opening are shown.

UCN production rate becomes 6 and 4 UCN/cm<sup>3</sup>/s, respectively, including multi-phonon excitation.

### 3.2.2 Experiments

For a storage time measurement, proton beam current of  $400 \text{ MeV} \times 0.2 \mu\text{A}$  impinged to the spallation target for 100 s. During proton beam impingement, a UCN valve (shown in Figure 1) was closed. After a timing delay  $\tau_d$ , the UCN valve was opened and number of UCN was counted by a UCN detector. In this test, an aperture disk with center hole of 1 cm in the diameter was installed in front of the UCN detector. Figure 2 shows the results. The counts during proton beam impingement arise from background neutrons and  $\gamma$ 's. UCN counts rise after valve opening and decay with a certain time constant. Since the aperture hole in front of the detector is small enough compared with the guide diameter, these decays arise from UCN loss in the UCN container.  $\tau_s$  was evaluated 47 s by these measurement.

We have estimated the UCN density  $\rho$  at the UCN valve by using the count rate just after valve opening. UCN count rate is represented by  $\frac{1}{4} \cdot v_{\text{av}} \cdot S \cdot \rho \cdot \epsilon$ , where  $v_{\text{av}}$  is an average velocity of UCN,  $S$  is a aperture disk hole cross-section and  $\epsilon$  is a detection efficiency of 0.68. Since the UCN valve is located 1.25 higher than UCN production point, the maximum energy of UCN is 90 neV and  $v_{\text{av}} = 3.1 \text{ m/s}$ . Figure 3 shows the UCN count rates. The proton beam power was  $400 \text{ MeV} \times 1 \mu\text{A}$ , and the proton irradiation time was increased up to 600 s. From this measurement, a UCN density of 15 UCN/cm<sup>3</sup>

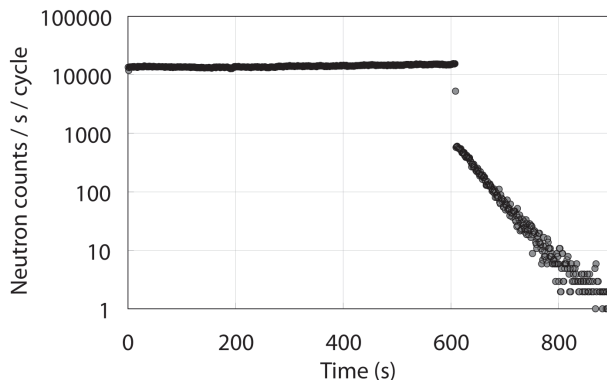


Figure 3: UCN counts. Proton beam of  $400 \text{ MeV} \times 1 \mu\text{A}$  was impinged for 600 s.

at the UCN valve with maximum energy of 90 neV was obtained. UCN with lower energy than 125 neV at the production point could not emerge from the vertical guide and are confined. Considering these confined UCN and enlargement of the momentum space at lower height, the total UCN number of  $1.4 \times 10^6$  was deduced. From this, UCN density of  $180 \text{ UCN/cm}^3$ , produced in the 8L of He-II, is obtained. Consequently, UCN production rate in He-II was determined to be  $4 \text{ UCN/cm}^3/\text{s}$  at maximum energy of 210 neV and the storage time of 47 s.

$\tau_s$  is limited by wall loss. We have decrease this wall loss by means of improvement of a surface condition. After alkali cleaning and high temperature baking ( $140^\circ\text{C}$ ),  $\tau_s$  increased 81 s shown in Figure 4. Since UCN density is proportional to  $\tau_s$ , UCN density is calculated to be  $26 \text{ UCN/cm}^3$  at the UCN valve and  $310 \text{ UCN/cm}^3$  at the UCN bottle.

### 3.3 Cryogenics

The temperature of He-II is determined by a balance of heat load on He-II and a cooling power of the cryostat. He-II temperature is kept by heat exchange with  $^3\text{He}$ . After the thermal equilibrium, super fluid film flow and a thermal radiation are the main component of the heat load.

During proton beam impingement, an extra heat load is come from a neutron-capture gamma heating. We have measured He-II and  $^3\text{He}$  temperature during UCN production by using Lakeshore cernox thermometer. The heat load of  $^3\text{He}$  was estimated by measuring  $^3\text{He}$  evaporated gas flow using

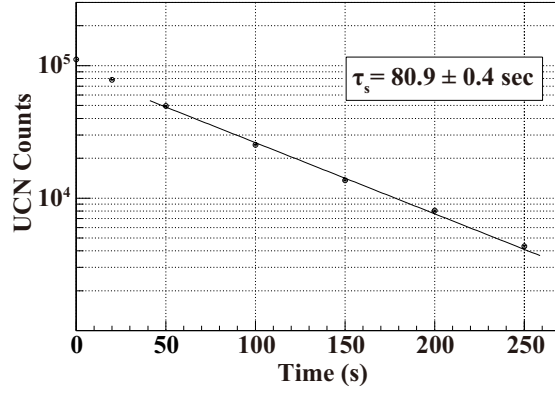


Figure 4: Storage time after alkali cleaning and high temperature baking. The UCN counts for 0, 25, 50, 100, 150, 200, and 250 s delay time of UCN valve opening after proton beam was stopped are shown.

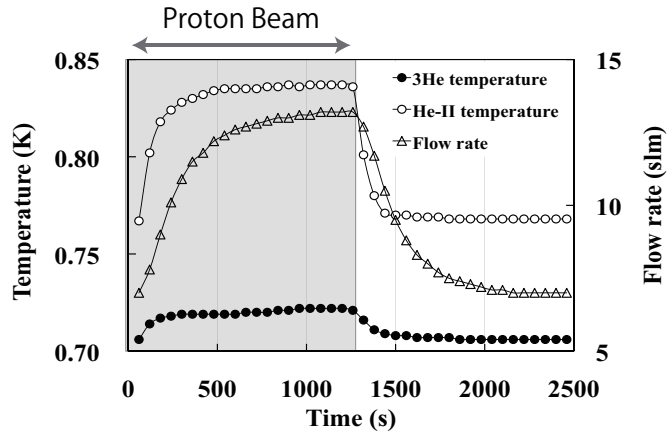


Figure 5: Cryogenics test. He-II and <sup>3</sup>He temperature transition by 1200 s proton beam impingement. <sup>3</sup>He flow rate is also described.

by KOFLOC mass-flow meter in the <sup>3</sup>He gas circulation line. The result is shown in Figure 5. The proton beam power is 400 MeV × 1 μA, and its duration times is 1200 s. The He-II temperature gradually rise up from 0.77 K to 0.83 K. After proton beam duration, the temperature return slowly to 0.77 K. <sup>3</sup>He temperature change similarly. The heat is exchanged from He-II to <sup>3</sup>He and rise up <sup>3</sup>He temperature. When <sup>3</sup>He temperature rise up, more

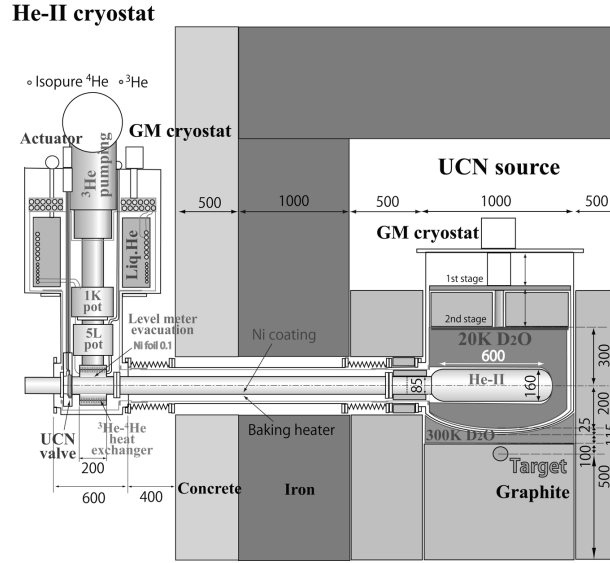


Figure 6: New UCN source

$^3\text{He}$  is evaporated and takes heat away. Then the temperature and  $^3\text{He}$  flow is balanced at certain point.

If we use a more effective heat exchanger, the temperature difference of He-II and  $^3\text{He}$  become much small and keep super-fluid He temperature lower.

## 4 Next UCN source at RCNP

A new UCN source has been developed. A main improvement is horizontal extraction of UCN shown in Figure 6. Avoiding gravity potential, all UCN can be extracted from He-II in spite of their energy. Furthermore, the horizontal straight guide improve their conductance. By the Monte Carlo simulation, 2.5 times more UCN can be extracted in the horizontal extraction guide.

Layout of the  $\text{D}_2\text{O}$  moderator and the spallation target is also optimized by the PHITS simulation. 1.2 times as much cold neutron flux will be available in the new layout. In addition, the volume of the superfluid helium is increased 1.5 times. With these improvements, the UCN density will be five times as much as the former UCN source.

A new He cryostat is also improved. It has a effective heat exchanger

with the surface area of 8 times as large as former one. A conductance of the He gas pumping line is also improved. Using this new cryostat, more proton current can be received without He-II temperature raising.

The D<sub>2</sub>O moderators and He cryostat have already installed at RCNP. First UCN production is plan to be 2013.

## 5 Summary

A spallation UCN source is developed at RCNP, Osaka University, Japan. UCN density of 26 UCN/cm<sup>3</sup> with maximum energy of 90 neV and storage time of 81 s is achieved. A new UCN source is now developing. With its geometrical improvement, 5 times as much UCN will be available in this source at same proton power.

## References

- [1] *R. Golub, D.J. Richardson, S.K. Lamreaux, // Ultra-Cold Neutrons, Hilger, (1991)*
- [2] *C.A. Baker D.D. Doyle, P. Geltenbort et al.// Phys. Rev. Lett. 97 (2006) 131801*
- [3] *V.V. Nesvizhevsky, H.G. Borner, A.M. Gagarski et al. // Nature, 415 (2002) 297*
- [4] *A. Serebrov, V. Varlamov, A. Kharitonov et al. // Phys. Lett. B 605 (2005) 72*
- [5] *R. Golub and J. Pendlebury // Phys. Lett. A 62 (1977) 337*
- [6] *Y. Masuda, K. Kitagaki, K. Hatanaka et al. // Phys. Rev. Lett. 89 (2002) 134801*
- [7] *Y. Masuda, K. Hatanaka, S.C. Jeong et al. // Phys. Rev. Lett. 108 (2012) 134801*
- [8] *E.Korobkina, R. Golub, B. Wehring and A. Young // Phys. Lett. A 301 (2002) 462*
- [9] *K. Inoue // J. Nucl. Sci. Technol., 7 (1970) 580*